Tunable Lumped Element Filters With BST Thin-Film Varactors

Errikos Lourandakis [#1], Matthias Schmidt [*2], Stefan Seitz [*3], Robert Weigel [#4]

[#]*Institute for Electronics Engineering, University of Erlangen-Nuremberg*
Cauerstrasse 9, D–91058 Erlangen, Germany
[1,4]{lourandakis,weigel}@lfte.de

[*]*EPCOS AG, R&D New Products Department*
Anzinger Strasse 13, D–81671 Munich, Germany

***Abstract*— Tunable lumped element filter topologies are discussed based on ferroelectric thin-film varactors. The design methodology for the proposed filter topologies relies on already known techniques and is enhanced with the tuning functionality by introducing the Barium-Strontium-Titanate (BST) varactors. Prototype circuits of a lowpass and a bandstop filter were fabricated and the measurement results showed good agreement to the corresponding calculated data. The lowpass prototype achieves a continuous tuning range from 1.5 GHz to 1.9 GHz. The highest measured passband insertion loss is about 4 dB and the input matching is better than -15 dB for all bias states. The implemented bandstop filter allows a continuous tuning of the notch frequency from 1.5 GHz to 2.1 GHz with a minimum attenuation of 17 dB.**

I. Introduction

Ferroelectric materials have been used in microwave applications for many decades. Nevertheless, the continuous progress in material compositions, manufacture- and assembly techniques reinforced the research activities over the last years. Thus a whole new family of microwave systems with tunable or frequency agile characteristics have been introduced, e.g. filters [1], [2], phase shifters [3], and matching networks [4]. Especially for mobile communications and their hand held user devices, the trend is clearly moving toward an increased number of communication bands. Reconfigurable systems, as they can be implemented with ferroelectric components, could enable new system architectures with a reduced number of functional blocks. Barium-Strontium-Titanate is probably the most promising ferroelectric material for such applications due to its high permittivity and well known RF-performance. In this work the used ferroelectric BST thin-film varactors are discussed in section II. The design procedure for tunable lumped element lowpass and bandstop filters is presented in section III. Transmission and reflection network parameters are analytically derived from the lumped element values, thus allowing parametric calculations. Prototype circuits were implemented and characterized by S-parameter measurements, in order to verify the suitability of the proposed methodology. The measurement results show good agreement to the calculated data and are presented in section IV.

II. Ferroelectric Thin-Film Varactors

Ferroelectric thin film varactors have the typical structure of metal-insulator-metal (MIM) capacitors. The ferroelectric film of height d is located between two metal electrodes and together they form a parallel plate capacitor. By applying a DC bias voltage V on the metal electrodes, an electrical field $\vec{E}$ is created. This field, given as E=V/d, causes a variation of the permittivity ε_r in the BST-film [5] and thus a voltage dependent capacitance. The overall electrical behavior of BST thin-film varactors can be modeled accurately [6], as indicated in Fig. 1. The measurements were taken with an Agilent

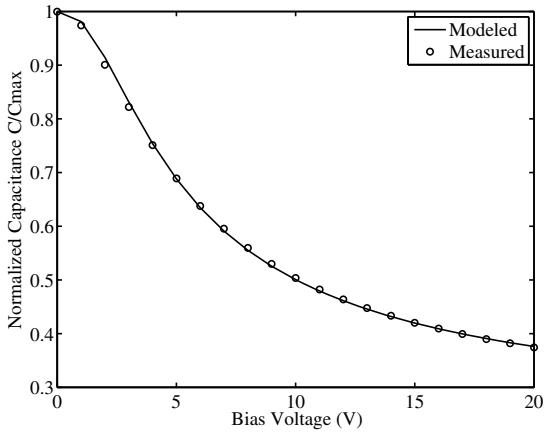

Fig. 1. Measured and modeled voltage dependent capacitance of a BST-varactor with zero bias capacitance of 5 pF.

E4991A RF-impedance analyzer after appropriate calibration. The capacitance value C is extracted from the measured input admittance Y according to (1).

$$C = \frac{\Im\{Y\}}{2\pi f} \tag{1}$$

The tunability, which is defined as $(\varepsilon_{rmax} - \varepsilon_{rmin})/\varepsilon_{rmax}$ exceeds 60 % for bias voltages up to 20 V.

III. FILTER DESIGN

Filter design methodologies based on different lowpass prototypes have been derived analytically in the past [7]. Transformations with closed formulas result in other high pass, bandpass or bandstop filter topologies. For the lumped element approach, the reactive elements insert poles or zeros to the network transfer function. By introducing tunable components, e.g. BST-varactors, an additional tuning functionality is achieved. The allocation of the inserted poles or zeros can be shifted and thus the resulting pass- or stop band characteristic altered. On the other hand, additional biasing components might be needed, which increase the overall circuit complexity and associated losses.

A. Lowpass Filter

The schematic of a tunable 5^{th}-order Chebyshev lowpass filter is shown in Fig. 2, where the initial capacitors were substituted by BST-varactors. Additional biasing components such as DC-block capacitors and one RF-choke inductor are incorporated in order to establish the proper biasing conditions for the ferroelectric varactors.

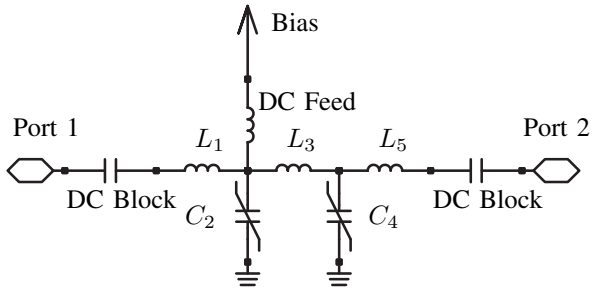

Fig. 2. Tunable 5^{th}-order lowpass filter with L_1=L_5≠L_3 and C_2=C_4=C.

Computing the network $ABCD$ parameters results in simply multiplying the chain matrices for all series and shunt branches.

$$M_{i=1,3,5} = \begin{bmatrix} A & B \\ C & D \end{bmatrix} = \begin{bmatrix} 1 & Z_i \\ 0 & 1 \end{bmatrix} \tag{2}$$

$$M_{j=2,4} = \begin{bmatrix} A & B \\ C & D \end{bmatrix} = \begin{bmatrix} 1 & 0 \\ Y_j & 1 \end{bmatrix} \tag{3}$$

For the ideal case, where the blocking capacitors represent a short circuit and the RF-choke inductor an ideal open, the circuit is reduced to the original 5^{th}-order topology. All series branches with inductive impedance of Z_i=pL_i can be represented with the chain matrix in (2). Respectively, all shunt branches with capacitive admittance of Y_j=pC_j can be described with the chain matrix in (3). In both cases, p=$\jmath\omega$ is the complex angular frequency. The resulting $ABCD$ matrix M_{total}=$M_1 \cdot M_2 \cdot M_3 \cdot M_4 \cdot M_5$ is used to calculate analytically the transmission and reflection scattering parameters of the network. For port impedances of Z_0, the ratio between reflection and transmission S-parameters is given as

$$\begin{aligned} \frac{S_{11}(p)}{S_{21}(p)} &= \frac{1}{2Z_0}p^5 L_1^2 L_3 C^2 + \\ & p^3\left(\frac{1}{Z_0}L_1^2 C + \frac{1}{Z_0}L_1 L_3 C - \frac{Z_0}{2}L_3 C^2\right) + \\ & p\left(-Z_0 C + \frac{1}{2Z_0}L_3 + \frac{1}{Z_0}L_1\right). \end{aligned} \tag{4}$$

The resulting conjugate complex zeros, which are the roots of the polynomial, are located at z_1=0 and

$$z_2 = \jmath\omega_2 = \pm\frac{\sqrt{2CL_3(-2L_1L_3 - 2L_1^2 + Z_0^2 CL_3 + \alpha)}}{2CL_1L_3} \tag{5}$$

$$z_3 = \jmath\omega_3 = \pm\frac{\sqrt{2CL_3(-2L_1L_3 - 2L_1^2 + Z_0^2 CL_3 - \alpha)}}{2CL_1L_3} \tag{6}$$

with the constant α given as

$$\alpha = \sqrt{-4L_1L_3^2Z_0^2C + 4L_1^4 + 4L_1^2L_3Z_0^2C + L_3^2Z_0^4C^2}. \tag{7}$$

These three discrete frequency points, where the reflection tends toward zero, are readily seen in the calculated response of an ideal filter in Fig. 3. The frequency response of the filter can be altered by changing the capacitance value C and thus shifting the network zero locations. For real implementations a performance degradation is expected, since the calculations apply for lossless elements and ignore additional biasing components. Nevertheless, the potential of implementing a frequency agile filter is clearly demonstrated. Such filters can be used in multi band transceivers of mobile radios in order to serve as an output filter for the power amplifier. Each supported frequency band could be covered separately since the BST-varactors allow a continuous tuning. Each bias setting would result in a different operating frequency.

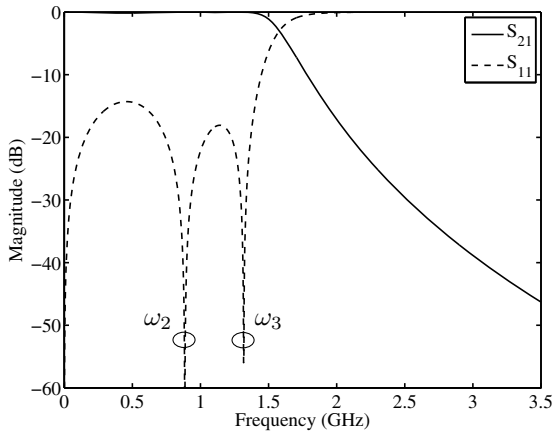

Fig. 3. Calculated S-parameters for an ideal 5^{th}-order lowpass filter with C=3 pF, L_1=L_5=6.8 nH, and L_3=12 nH.

B. Bandstop Filter

Bandstop or notch filter topologies can be derived from the discussed lowpass prototypes by a simple substitution of the shunt capacitive branches with series LC resonators. The

series inductive branches are then substituted by parallel LC resonators. A first order tunable bandstop filter is depicted in Fig. 4. Two cascaded capacitors are used, instead of a single one, in order to simplify the bias supply and avoid additional DC-block capacitors.

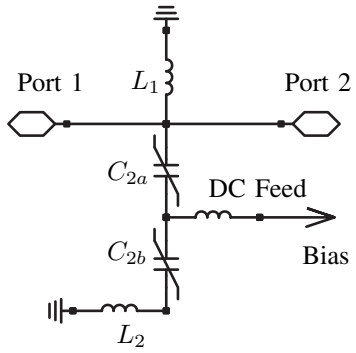

Fig. 4. Tunable bandstop filter with cascaded BST-varactors C_{2a}=C_{2b}=C.

Applying the same principle as before, the transfer function of the network can be computed by multiplying the individual $ABCD$ matrices.

$$M_1 = \begin{bmatrix} A & B \\ C & D \end{bmatrix} = \begin{bmatrix} 1 & 0 \\ Y_1 & 1 \end{bmatrix} \tag{8}$$

$$M_2 = \begin{bmatrix} A & B \\ C & D \end{bmatrix} = \begin{bmatrix} 1 & 0 \\ Y_2 & 1 \end{bmatrix} \tag{9}$$

The overall network transfer function is M_{total}=$M_1 \cdot M_2$. In (8) the shunt admittance in the first branch is Y_1=$1/pL_1$ whereas in (9) the admittance of the second branch is calculated, from the series combination of the inductor and the two cascaded capacitors, as Y_2=$1/[(2/pC) + pL_2]$. The analytical expressions for the reflection and transmission S-parameters can be calculated from the overall $ABCD$ matrix of the network. For port impedances of Z_0, the ratio between them is then given as

$$\frac{S_{11}(p)}{S_{21}(p)} = -\frac{Z_0}{2} \cdot \frac{2 + p^2 C(L_1 + L_2)}{pL_1(2 + p^2 L_2 C)}. \tag{10}$$

Network parameters such as poles and zeros are readily extracted from (10). The conjugate complex network zeros, which are the roots of the numerator, are located at z_1=$\jmath\omega_1$=$\pm(\sqrt{-2/(L_1 + L_2)C})$. The corresponding conjugate complex poles, which are roots of the denominator, are located at p_1=0 and p_2=$\jmath\omega_2$=$\pm\sqrt{-2/L_2C}$.

Changing the capacitance value C results in shifting the zero and pole frequency and thus the pass- and stopband allocation respectively, as illustrated in Fig. 5. Shifting the notch frequency could be used in order to suppress crosstalk signals within the receiver or to block strong interferers. These unwanted scenarios reduce the sensitivity of the receiver and thus the overall radio front-end efficiency. Again, a real implementation with lumped finite-Q elements would result in performance degradation.

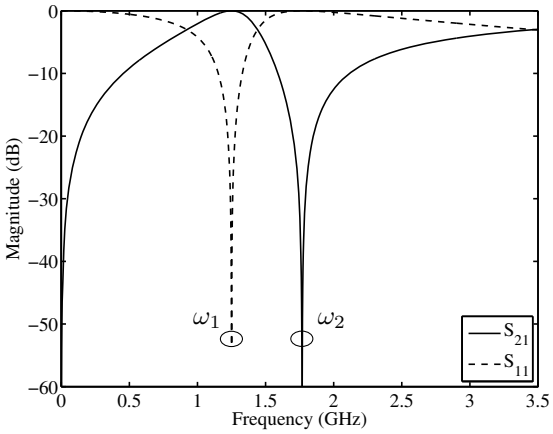

Fig. 5. Calculated S-parameters for an ideal notch filter with C=6 pF and L_1=L_2=2.7 nH.

IV. Prototype implementation and Measurements

Both previously discussed filter topologies were implemented as prototype boards on a Rogers RO3010 substrate (h=0.625 mm and ε_r=10.2) and are illustrated in Fig. 6. The actual footprint for both circuits consists only of 0402-series SMD components and the BST-varactors. The additional feeding microstrip lines serve for the bias and to mount the coaxial SMA connectors. The ferroelectric varactors were assembled in a flip-chip procedure in order to minimize the interconnection parasitics and the associated loss mechanisms for higher operating frequencies. Gold stud bumps were placed on the varactor chip pads and connected to the board metal traces via a conductive adhesive. All measurements were taken with a Rohde & Schwarz ZVB8 vector network analyzer.

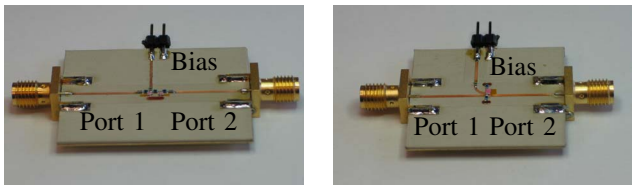

(a) Lowpass filter (b) Bandstop filter

Fig. 6. Fabricated prototype boards.

A. Lowpass filter

The measured transmission and reflection S-parameters of the lowpass prototype with C=3 pF, L_1=L_5=6.8 nH, and L_3=12 nH are shown in Fig. 7. The operating frequency can be tuned from 1.5 GHz to 1.9 GHz with a maximum insertion loss of about 4 dB in the passband. The high losses are due to moderate quality factors of the BST-varactors in the higher frequency region. The input matching remains below -15 dB for all operating bias states. As predicted by the previous analysis, the filter passband characteristic is shifted toward higher frequencies for higher bias voltages. This is achieved

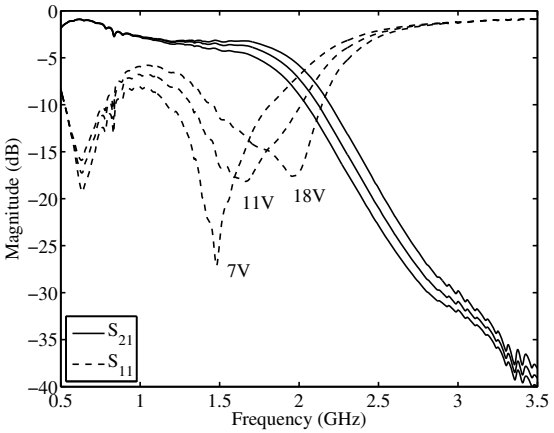

Fig. 7. Measured transmission and reflection S-parameters for the lowpass prototype at different bias states.

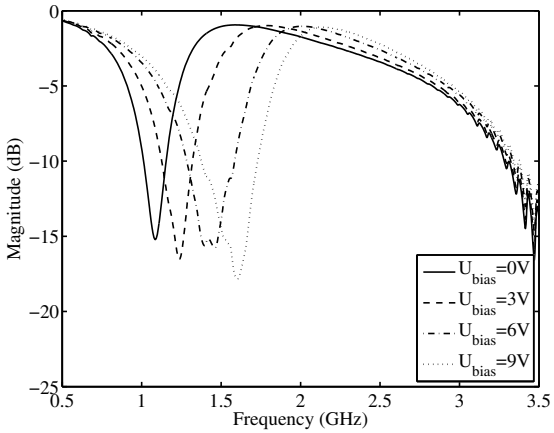

Fig. 9. Measured S_{11} reflection S-parameter for bandstop filter at different bias states.

by altering the capacitance value C and therefore the zero allocation of the filter, as can be seen in (5) – (7).

B. Bandstop filter

The measured transmission parameter S_{21} and reflection parameter S_{11} for the implemented notch filter, with C=5 pF and inductor values of L_1=L_2=2.7 nH, are presented in Fig. 8 and Fig. 9 respectively. A continuously tunable stopband filtering is achieved from 1.5 GHz to 2.1 GHz with a minimum attenuation of 17 dB. The return loss for each operating state is not exceeding 1.1 dB within the stopband bandwidth. Thus selective filtering of unwanted blocking signals is possible in this frequency region.

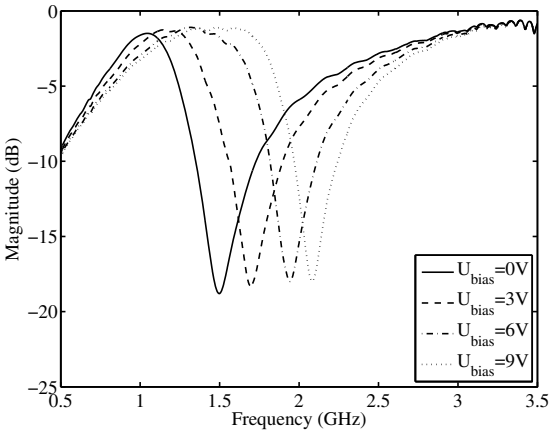

Fig. 8. Measured S_{21} transmission S-parameter for bandstop filter at different bias states.

As expected, the pole and zero allocation of the filter is shifted toward higher frequencies by raising the bias voltage and thus decreasing the capacitance value of the BST-varactor.

V. Conclusions

Tunable filter topologies based on lumped elements and BST-varactors are discussed. Analytical formulas are derived for the transmission and reflection network parameters of a lowpass and a bandstop filter from the corresponding circuit parameter values. The principle of using ferroelectric varactors for altering the filter characteristics was demonstrated with two prototype boards. The measurement results reveal the potential of such topologies to operate as frequency agile solutions in reconfigurable front-end architectures. The implemented prototype filters operate in the frequency region from 1.5 GHz to 2 GHz and thus enable multi band operation in front-end systems.

Acknowledgment

This work was conducted within the MARIO project (FKZ 01BU570) which is funded and supported by the federal ministry of education and research (BMBF) in Germany.

References

[1] A. Tombak, F. Ayguavives, J.-P. Maria, G. Stauf, A. Kingon, and A. Mortazawi, "Tunable RF Filters using Thin Film Barium Strontium Titanate based Capacitors," in *2001 IEEE MTT-S Int. Microwave Symp. Dig.*, vol. 3, 20–25 May 2001, pp. 1453–1456.

[2] J. Nath, D. Ghosh, J. Maria, A. Kingon, W. Fathelbab, P. Franzon, and M. Steer, "An electronically tunable microstrip bandpass filter using thin-film Barium-Strontium-Titanate (BST) varactors," *IEEE Trans. Microwave Theory and Tech.*, vol. 53, no. 9, pp. 2707–2712, 2005.

[3] D. Kim, Y. Choi, M. Allen, J. Kenney, and D. Kiesling, "A wide-band reflection-type phase shifter at S-band using BST coated substrate," *IEEE Trans. Microwave Theory and Tech.*, vol. 50, no. 12, pp. 2903–2909, 2002.

[4] M. Schmidt, E. Lourandakis, A. Leidl, S. Seitz, and R. Weigel, "A Comparison of Tunable Ferroelectric Π and T-Matching Networks," in *Proc. 37th European Microwave Conf.*, 9–12 Oct. 2007, pp. 98–101.

[5] D. Chase, L. Chen, and R. York, "Modeling the Capacitive Nonlinearity in Thin-Film BST Varactors," *IEEE Trans. Microwave Theory and Tech.*, vol. 53, no. 10, pp. 3215–3220, 2005.

[6] M. Schmidt, E. Lourandakis, R. Weigel, A. Leidl, and S. Seitz, "A Thin-Film BST Varactor Model for Linear and Nonlinear Circuit Simulations for Mobile Communication Systems," in *2006 IEEE Int. Symposium on the Applications of Ferroelectrics*, 30 Jul.–3 Aug. 2006, pp. 372–375.

[7] G. Matthaei, L. Young, and E. Jones, *Microwave Filters, Impedance-Matching Networks, and Coupling Structures*. McGraw-Hill, 1964.